

Structural, Spectroscopic, Thermodynamic and Kinetic Properties of Copper(II) Complexes with Tripodal Tetraamines

Florian Thaler, Colin D. Hubbard, Frank W. Heinemann, Rudi van Eldik,* and Siegfried Schindler

Institute for Inorganic Chemistry, University of Erlangen–Nürnberg, Egerlandstrasse 1, 91058 Erlangen, Germany

István Fábián

Department of Inorganic and Analytical Chemistry, Lajos Kossuth University, 4010 Debrecen 10, Hungary

Andreas M. Dittler-Klingemann and F. Ekkehardt Hahn

Institute for Inorganic and Analytical Chemistry, Freie Universität Berlin, Fabeckstrasse 34–36, 14195 Berlin, Germany

Chris Orvig

Department of Chemistry, University of British Columbia, 2036 Main Mall, Vancouver, British Columbia V6T 1Z1, Canada

Received October 14, 1997

Spectroscopic, thermodynamic, and kinetic measurements have been made on aqueous solutions of copper(II) complexes of hexamethylated tren and trimethylated tren (one methylation per primary amine group of tren) with the objective of correlating the influence of geometry (trigonal bipyramidal, evident from UV/vis spectroscopy) and *N*-alkyl substitution in the ligand on these inherent properties. At 25.0 °C the protonation constants of Me₃tren are not significantly different from those of tren and Me₆tren, and the stability constant for the Cu(II) complex is of the same order of magnitude as that for the [Cu(tren)(H₂O)]²⁺ complex ion. The p*K*_a for deprotonation of the coordinated water molecule of [Cu(Me₃tren)(H₂O)]²⁺ is intermediate between the values for the complexes containing the unsubstituted and the fully substituted tren ligand. Substitution (pyridine for water) kinetics measurements employing stopped-flow and temperature-jump methods revealed different patterns of reactivity: pyridine replaces water in [Cu(Me₃tren)(H₂O)]²⁺ with a second-order rate constant of $(4.4 \pm 0.8) \times 10^2 \text{ M}^{-1} \text{ s}^{-1}$ at 25.0 °C, whereas the corresponding process for [Cu(Me₆tren)(H₂O)]²⁺ is relatively complex and is discussed in more detail. Substitution in the former complex ion is characterized in the forward and reverse directions, by $\Delta H^\ddagger = 60 \pm 8$ and $51.9 \pm 0.9 \text{ kJ mol}^{-1}$, $\Delta S^\ddagger = 5 \pm 27$ and $-23 \pm 3 \text{ J mol}^{-1} \text{ K}^{-1}$, and $\Delta V^\ddagger = -8.7 \pm 4.6$ and $-6.2 \pm 1.1 \text{ cm}^3 \text{ mol}^{-1}$, respectively. It is concluded that this reaction follows an I_a mechanism, similar to that reported for the comparable reaction of [Cu(tren)(H₂O)]²⁺. An X-ray structural determination on a crystal of [Cu₂(Me₃tren)₂(CN)](ClO₄)₃·2CH₃CN demonstrated trigonal bipyramidal geometry about each copper(II) center. As has been found in comparable complexes of tren and Me₆tren, the axial nitrogen to copper bond is shorter than the equatorial nitrogen–copper bonds, and the angle made by N(axial)–Cu–N(equatorial) is less than 90° (84.6–85.4°), signifying that each copper ion lies below the plane of the equatorial nitrogen atoms.

Introduction

In a previous paper¹ we have reported the molecular structures of [Cu(trpn)(NO₃)₂](NO₃)₂ and of [Cu(332)(NO₃)₂](NO₃)₂ (ligand abbreviations are given in Figure 1) and presented the thermodynamic parameters (protonation constants of the ligands and the stability constants of the complexes) and UV/vis spectra of the complexes, as well as these properties of the analogous

Cu^{II}(322) complex. These properties were compared and contrasted with those available for the Cu^{II}(tren) complex. The purpose of our previous study was to assess the influence of particular geometries in governing the magnitudes of these properties. Delineating these factors is important for a rational understanding of copper(II) or indeed of copper(I) chemistry in a range of bioinorganic systems (metalloproteins and metalloenzymes).² Principal findings were that when copper(II)

(1) Dittler-Klingemann, A. M.; Orvig, C.; Hahn, F. E.; Thaler, F.; Hubbard, C. D.; van Eldik, R.; Schindler, S.; Fábián, I. *Inorg. Chem.* **1996**, *35*, 7798.

(2) Karlin, K. D.; Tyeklár, Z. *Bioinorganic Chemistry of Copper*; Chapman & Hall: New York, 1993.

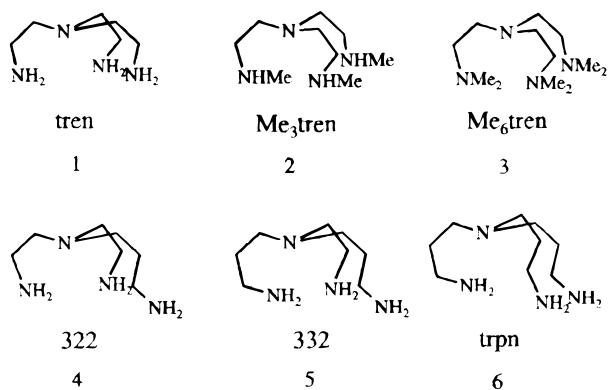


Figure 1. Tripodal tetraamine ligands.

nitrate in neutral aqueous solution reacts with either trpn or 322, the products crystallize to yield binuclear, square pyramidal copper(II) species. Two primary and the one tertiary amine groups coordinate to one copper center, and the remaining primary amine arm bridges to the second copper center. This geometry, supported by a visible spectrophotometric study and indirectly by potentiometry, is in contrast to the established tetragonal distorted trigonal bipyramidal structure of the mononuclear copper(II) complexes of tren, 322, 332, and trpn in which an ammonia ligand occupies the fifth (axial) position.^{3,4}

In this contribution we extend this subject to consider the copper(II) complexes of 2,2',2''-tris(dimethylamino)triethylamine (Me₆tren) and 2,2',2''-tris(monomethylamino)triethylamine (Me₃tren). Structural aspects and thermodynamic properties of the ligands, of the complexes, and of the coordinated water molecule in the complex copper(II) ions are reported. The lability of the complex ions has been investigated by employing rapid reaction methods.

Experimental Section

Materials. Except for the preparations reported below, compounds used were of commercially available reagent quality (Aldrich). Doubly distilled water was used for the preparation of the aqueous solutions. Sodium perchlorate was recrystallized from water.

WARNING! Perchlorate salts are potentially explosive. They should be handled in small amounts and with caution.

The ligand Me₆tren was prepared by a literature method⁵ and characterized by ¹³C and ¹H NMR spectroscopy. The spectra were in accord with those in the literature.⁶

The ligand Me₃tren was prepared by a literature method.⁷ The trihydroperchlorate salt was purified by recrystallization from ethanol–water mixtures. The elemental analyses of the trihydroperchlorate of the molecular formula C₉H₂₇N₄O₁₂Cl₃ (found/calculated (in percent)) are as follows: C, 22.21/22.07; H, 5.24/5.56; N, 11.51/11.44. The free ligand exhibited the same shifts in the ¹³C NMR spectrum as reported in the literature.⁷ The trihydroperchlorate salt of Me₃tren in D₂O gave ¹³C shifts of 46.5 (CH₂), 43.6 (CH₂), and 30.9 (CH₃) ppm with TSP as reference and ¹H values of 2.77 (9 H, s, CH₃), 2.93 (6 H, t, ³J_{HH} = 6.6 Hz), and 3.20 ppm (6 H, t, ³J_{HH} = 6.6 Hz), also with TSP as reference.

The [Cu(Me₆tren)(H₂O)]²⁺ and the [Cu(Me₃tren)(H₂O)]²⁺ complexes were prepared by mixing stoichiometric amounts of Cu(ClO₄)₂ and the respective ligands in water. Formation of the complexes was checked by UV/vis spectroscopy. The spectrum of the former complex ion was in excellent agreement with that obtained by dissolving the solid [Cu(Me₆tren)](ClO₄)₂ in water at the given pH,⁸ while the spectrum of the latter complex has not been established previously and is displayed and described below.

Methods. (a) Solution Studies. The thermodynamic and kinetic measurements were carried out at 25.0 ± 0.1 °C in 1.0 M NaClO₄. UV/vis spectra were obtained on a Varian Cary 5, on a Varian Cary 1 or on a Shimadzu 160 spectrophotometer using 1 cm quartz cells. ¹³C and ¹H NMR spectra were recorded on a Bruker DXP 300 AVANCE spectrometer. EPR measurements were performed on a Bruker ESP-300E spectrometer at 77 K. The EPR spectrum of [Cu(Me₃tren)](ClO₄)₂ was obtained in a frozen methanol–water mixture (9:1, v/v) at a concentration of 5.5 × 10⁻³ M. The pH of solutions was measured by employing a WTW PMX 500 pH meter with an Ingold combined glass electrode. The electrode calibration for H⁺ concentration was such that “pH” is defined as -log[H⁺]. The method has been described elsewhere.^{9,10}

(b) Determination of Ligand Protonation Constants. This was necessary only in the case of Me₃tren, as values for Me₆tren and tren had been determined earlier.¹¹ Me₃tren was titrated potentiometrically employing a Metrohm 702 SM Titrino instrument equipped with a Metrohm combination glass electrode (No. 6.0203.100). Potassium chloride electrode solution was replaced by 3.0 M sodium chloride solution. The temperature was maintained at 25.0 ± 0.1 °C by circulating fluid from a thermostated bath. Solutions were kept under an atmosphere of nitrogen. The electrode was calibrated by titrating a known amount of aqueous HClO₄ with an ionic strength of I = 1.0 M (NaClO₄) with a known quantity of NaOH (I = 1.0 M, NaClO₄). A Gran plot was performed to check for contamination of the solutions by CO₂. The stock solutions were discarded when the level of contamination was higher than 0.5%. A correction of the measured pH values to those calculated was taken into consideration for the calculations to determine the equilibrium constants. The pK_a values were obtained by treating the data with the PSEQUAD program.¹²

(c) Determination of Complex Stability Constants. (i) Me₆tren. The complex stability constant for substitution of water on [Cu(Me₆tren)(H₂O)]²⁺ by pyridine was determined in the following manner. The measurements were carried out at a pH of 6.00, 6.70, or 7.10 (always ±0.02) by adding various amounts of pyridine to a solution of 2.0 × 10⁻³ M [Cu(Me₆tren)(H₂O)]²⁺. According to earlier published stability constants of the Cu^{II}–Me₆tren system¹¹ at these pH values, [Cu(Me₆tren)(H₂O)]²⁺ is the predominant species in aqueous medium at 25.0 °C, prior to the addition of pyridine.

The stability constant of the [Cu(Me₆tren)(py)]²⁺ complex was calculated by simultaneously fitting the experimental data at seven different wavelengths between 670 and 850 nm with the program PSEQUAD. The thermodynamic data describing

(3) Duggan, M.; Ray, N.; Hathaway, B. *J. Chem. Soc., Dalton Trans.* **1980**, 1342.

(4) Dittler-Klingemann, A. M.; Hahn, F. E. *Inorg. Chem.* **1996**, *35*, 1996.

(5) Ciampolini, M.; Nardi, N. *Inorg. Chem.* **1966**, *5*, 41.

(6) Coates, J. H.; Collins, P. R.; Lincoln, S. F. *Aust. J. Chem.* **1980**, *33*, 1381.

(7) Schmidt, H.; Lensink, C.; Xi, S. K.; Verkade, J. G. *Z. Anorg. Allg. Chem.* **1989**, *578*, 75.

(8) Lincoln, S. F.; Hubbard, C. D. *J. Chem. Soc., Dalton Trans.* **1974**, 2513.

(9) Fábrián, I.; Diebler, H. *Inorg. Chem.* **1987**, *26*, 925.

(10) Diebler, H.; Rosen, P. *Ber. Bunsen-Ges. Phys. Chem.* **1972**, *76*, 1031.

(11) Anderegg, G.; Gramlich, V. *Helv. Chim. Acta* **1994**, *77*, 685.

(12) Zekány, L.; Nagypál, I. In *Computational Methods for the Determination of Formation Constants*; Leggett, D. J., Ed.; Plenum Press: New York, 1985; p 291.

the $\text{Cu}^{\text{II}}-\text{py}$ system, needed for the calculations, were taken from the literature.¹³

The spectra of the $\text{Cu}^{\text{II}}-\text{pyridine}$ species were obtained by titrating hexaaqua $\text{Cu}(\text{II})$ ions with pyridine at a pH of 6.00 ± 0.02 and an ionic strength of $I = 1.0 \text{ M}$ (NaClO_4). Since $[\text{Cu}(\text{py})_4](\text{ClO}_4)_2$ has a low solubility, its spectrum could not be established with a high degree of precision. Therefore nitrate salts were used for determining the spectra of $[\text{Cu}(\text{py})_3]^{2+}$ and $[\text{Cu}(\text{py})_4]^{2+}$, with the implicit assumption that the anion has no influence on the wavelength or absorptivity of the species in question.

(ii) Me_3tren . Similar procedures as for the hexamethyl analogue were used. The equilibrium constants for the formation of $[\text{Cu}(\text{Me}_3\text{tren})(\text{H}_2\text{O})]^{2+}$ and that governing the deprotonation of $[\text{Cu}(\text{Me}_3\text{tren})(\text{H}_2\text{O})]^{2+}$ were determined potentiometrically, while that for the displacement of coordinated water by pyridine was determined spectrophotometrically using multiple wavelength absorbance values in the 670–850 nm region, in a manner parallel to that described above.

(d) Kinetics. Kinetic investigations of the substitution of $[\text{Cu}(\text{Me}_6\text{tren})(\text{H}_2\text{O})]^{2+}$ by pyridine were performed either in tandem cuvettes with a path length of 0.88 cm, thermally equilibrated at $25.0 \pm 0.1 \text{ }^\circ\text{C}$, before mixing in a Shimadzu CPS thermostat, or in the BIO-LOGIC stopped-flow SFM-3 instrument (also thermostated at $25.0 \pm 0.1 \text{ }^\circ\text{C}$) with a 1 cm path length at wavelengths of 340, 780, and 840 nm. The pH was adjusted with 0.050 M MES (3-[*N*-morpholino]ethanesulfonic acid) and NaOH to 6.00 ± 0.02 , and the ionic strength was adjusted to 1.0 M with NaClO_4 . The kinetic traces were recorded by using an on-line computer and treated with the OLIS KINFIT program (Bogart, GA).¹⁴

The rate of substitution of H_2O by pyridine in the aqua $\text{Cu}(\text{II})$ complex of Me_3tren is such that it may be monitored in either a stopped-flow spectrophotometer with a few milliseconds dead-time (Applied Photophysics model SX.18MV) thermostated over the range of 5–25 $^\circ\text{C}$ or in a temperature-jump instrument (Messanlagen, Göttingen).¹⁵ The latter was chosen for high-pressure kinetics (up to 140 MPa) as the time resolution of our high-pressure stopped-flow spectrophotometer would be insufficient to permit meaningful measurements.¹⁶ The measurements were carried out on solutions of pH 7.10 ± 0.02 (0.050 M MOPS (3-[*N*-morpholino]propanesulfonic acid)) and $I = 1.0 \text{ M}$ (NaClO_4). The stopped-flow measurements were made at 340 nm and 25.0 $^\circ\text{C}$, and the data were processed as indicated above. A temperature jump of 3 $^\circ\text{C}$ was applied to solutions thermostated at 22 $^\circ\text{C}$. Relaxation was monitored in the 310–340 nm range, but mostly at 328 nm, with at least 10, and up to 25, replicate traces being processed as reported earlier.^{17,18}

Results and Discussion

(a) Structural Studies. To determine the geometry of the $[\text{Cu}(\text{Me}_3\text{tren})]^{2+}$ ion in the solid-state several attempts were made to obtain the X-ray structure of the aquo or pyridine complex. Suitable crystals of these complexes for structure determination could not be obtained. However, we were successful in preparing the binuclear $[\text{Cu}_2(\text{Me}_3\text{tren})_2(\text{CN})]-$

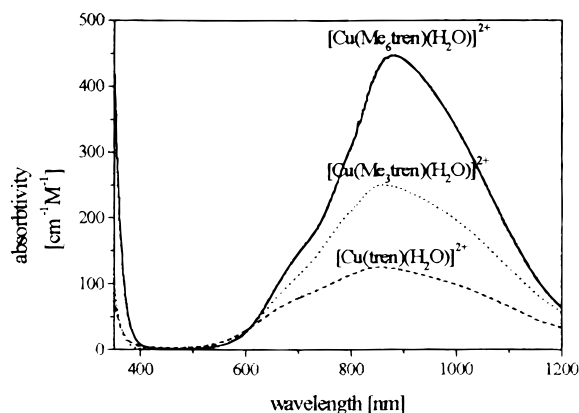


Figure 2. Room-temperature vis-NIR spectra of $[\text{Cu}(\text{tren})(\text{H}_2\text{O})]^{2+}$, $[\text{Cu}(\text{Me}_3\text{tren})(\text{H}_2\text{O})]^{2+}$, and $[\text{Cu}(\text{Me}_6\text{tren})(\text{H}_2\text{O})]^{2+}$ in water.

$(\text{ClO}_4)_3 \cdot 2\text{CH}_3\text{CN}$ complex in a form amenable to X-ray structure determination. Indeed it shows retention of the trigonal bipyramidal geometry in the solid state. The structure itself is discussed in more detail in the Supporting Information.

(b) Solution Studies. (i) UV/Vis Spectroscopy. The UV/vis spectra of $[\text{Cu}(\text{Me}_6\text{tren})(\text{H}_2\text{O})]^{2+}$ and $[\text{Cu}(\text{tren})(\text{H}_2\text{O})]^{2+}$ (pH of 6.00 and 7.10, and $I = 1.0 \text{ M}$ (NaClO_4)) are consistent with the published spectra^{1,8} and are indicative of trigonal bipyramidal geometry since a maximum at 880 nm and a shoulder in the region of 700 nm for $[\text{Cu}(\text{Me}_6\text{tren})(\text{H}_2\text{O})]^{2+}$ and a maximum at 850 nm for $[\text{Cu}(\text{tren})(\text{H}_2\text{O})]^{2+}$ were observed. Copper(II) complex geometries have been thoroughly characterized by means of UV/vis spectra.^{3,19,20} The X-ray structure of $[\text{Cu}(\text{Me}_6\text{tren})(\text{H}_2\text{O})]^{2+}$ supports this geometry.²¹

The UV/vis spectrum of $[\text{Cu}(\text{Me}_3\text{tren})(\text{H}_2\text{O})]^{2+}$ at pH 7.10 and $I = 1.0 \text{ M}$ (NaClO_4) is illustrated in Figure 2. Once again the maximum at 860 nm and the shoulder in the region of 700 nm point toward trigonal bipyramidal geometry for the solution species. The wavelength at the maximum is 860 nm compared with 880 nm for $[\text{Cu}(\text{Me}_6\text{tren})(\text{H}_2\text{O})]^{2+}$ and 850 nm for $[\text{Cu}(\text{tren})(\text{H}_2\text{O})]^{2+}$, which indicates that all three complexes have a very similar geometry. The molar absorptivity at the maximum varies widely (Figure 2). It is difficult to correlate these results quantitatively with specific features,²² but they may indicate an increasing distortion of the complex geometry due to the bulkiness of the methyl groups.

(ii) EPR Measurements. The EPR spectrum of $[\text{Cu}(\text{Me}_3\text{tren})](\text{ClO}_4)_2$ in methanol–water (9:1, v/v) with $g_{\perp} = 2.209 > g_{\parallel} = 2.014$, and $A_{\perp} = 105.7 \text{ cm}^{-1}$ provides additional verification of the trigonal bipyramidal geometry of the complex in solution. g_{\parallel} is slightly higher than the values mostly found for trigonal bipyramidal copper(II) complexes with $g_{\parallel} = g_e = 2.0023$.²³ $[\text{Cu}(\text{Me}_6\text{tren})]^{2+}$ in water also exhibits a higher value ($g_{\parallel} = 2.011$) than the free electron g factor.²⁴ An explanation might be that there is a small but significant admixture of d_{xy} or $d_{x^2-y^2}$ orbitals into the ground state via vibronic coupling.²⁴ Figure 3 illustrates that the expected hyperfine splitting due to an $I = 3/2$ nuclear spin of copper(II) is well resolved in the g_{\perp} region.

(iii) Potentiometric Titrations. Table 1 reports the protonation constants of Me_3tren ; for comparison the nonmethylated

(13) Atkinson, G.; Bauman, J. E. *Inorg. Chem.* **1963**, *2*, 64.

(14) OLIS KINFIT, Bogart, GA.

(15) Doss, R.; van Eldik, R.; Kelm, H. *Rev. Sci. Instrum.* **1982**, *9*, 715.

(16) van Eldik, R.; Gaede, W.; Wieland, S.; Kraft, J.; Spitzer, M.; Palmer, D. A. *Rev. Sci. Instrum.* **1993**, *64*, 1355.

(17) Powell, D. H.; Merbach, A. E.; Fábíán, I.; Schindler, S.; van Eldik, R. *Inorg. Chem.* **1994**, *33*, 4468.

(18) Projahn, H. D.; Schindler, S.; van Eldik, R.; Fortier, D. G.; Andrew, C. R.; Sykes, A. G. *Inorg. Chem.* **1995**, *34*, 5935.

(19) Hathaway, B. In *Comprehensive Coordination Chemistry*; Wilkinson, G., Ed.; Pergamon: New York, 1987; Vol. 5, pp 533–777.

(20) Hathaway, B.; Billing, D. E. *Coord. Chem. Rev.* **1970**, *5*, 143.

(21) Lee, S. C.; Holm, R. H. *J. Am. Chem. Soc.* **1993**, *115*, 11789.

(22) Lever, A. B. P. In *Inorganic Electronic Spectroscopy*, 2nd ed.; Elsevier: Amsterdam, 1984; p 174.

(23) Barbucci, R.; Bencini, A.; Gatteschi, D. *Inorg. Chem.* **1977**, *16*, 2117.

(24) Barbucci, R.; Campbell, M. J. M. *Inorg. Chim. Acta* **1975**, *15*, L15.

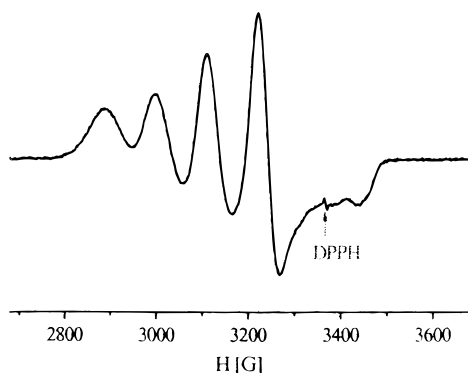


Figure 3. EPR spectrum of $[\text{Cu}(\text{Me}_3\text{tren})](\text{ClO}_4)_2$ in a frozen methanol–water (9:1, v/v) mixture.

Table 1. Protonation Constants of the Ligands (25.0 ± 0.1 °C, $I = 1.0$ M (NaClO_4))^a

ligand	log K_1	log K_2	log K_3	log K_4	ref
tren	10.42(1)	9.88(1)	8.915(5)	<1	11
Me_3tren	10.93(1)	10.24(1)	9.17(1)	<1	this work
Me_6tren	10.13(1)	9.32(1)	8.17(1)	<1	11

^a Numbers in parentheses are the standard deviations in the last digit.

Table 2. Stability Constants (log K_{ML}) and $\text{p}K_{\text{a}}$ Values of the Coordinated Water Molecule of the Copper Complexes ML^{2+} (25.0 ± 0.1 °C, $I = 1.0$ M (NaClO_4))^{a,b}

complex	log K_{ML}	$\text{p}K_{\text{a}}$	ref
$[\text{Cu}(\text{tren})(\text{H}_2\text{O})]^{2+}$	19.58(3)	9.4	11
$[\text{Cu}(\text{Me}_3\text{tren})(\text{H}_2\text{O})]^{2+}$	19.11(2)	9.08(2)	this work
$[\text{Cu}(\text{Me}_6\text{tren})(\text{H}_2\text{O})]^{2+}$	15.65(3)	8.1	11

^a With the program PSEQUAD we could not obtain reasonable results for the protonated species MLH^{3+} , because this species, if it exists, is formed only in infinitely small amounts. ^b Numbers in brackets are the standard deviations in the last digit.

ligand tren and the hexamethylated tren are listed. *N*-Methyl substitution only modestly affects the ease or difficulty of protonation ($\text{tren}/\text{Me}_3\text{tren}/\text{Me}_6\text{tren}$).

Stability constants for the copper(II) aqua complexes of the three “tren” ligands are listed in Table 2. Intuitively one expects the methylation of tren to reduce the donor strength of the nitrogen atoms by a steric effect, less so for monomethylation at each nitrogen, and indeed this is the case, as shown in Table 2. An additional consequence of the lower donor strength is the slight decrease in the $\text{p}K_{\text{a}}$ values of the coordinated water. Table 2 contains the relevant $\text{p}K_{\text{a}}$ values along with that for the hexaqua copper(II) ion.

(iv) Spectrophotometric Titrations. As pyridine solution is added to the aqua copper(II) complex of Me_6tren , at either pH 6.00, 6.70, or 7.10, the pronounced peak at 875 nm is incrementally reduced. Further aliquots of pyridine reduce the absorbance virtually completely. This change is accompanied by an increase in absorbance in the region of 580 nm. These observations can be attributed to the formation of the ultimate products, copper(II) pyridine complexes, since it will be shown that the UV/vis spectrum of the $[\text{Cu}(\text{Me}_6\text{tren})(\text{py})]^{2+}$ complex ion is not distinguishable from that of the aqua complex. In the pH range specified, the latter complex, before addition of pyridine, is present virtually entirely as the aqua complex ion (i.e. no deprotonation) since the corresponding $\text{p}K_{\text{a}}$ is 8.1. To calculate the concentrations of any species present under the pertinent conditions for either equilibrium or kinetics experiments, it is necessary to assemble all the possible species present, together with the equilibrium constants relevant to each equi-

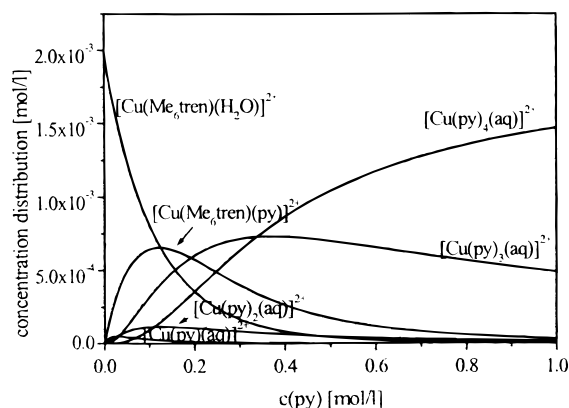


Figure 4. Speciation diagram for $[\text{Cu}(\text{Me}_6\text{tren})(\text{H}_2\text{O})]^{2+}$ and py as a function of the total pyridine concentration (25.0 °C, $\text{pH} = 6.00$, $I = 1.0$ M (NaClO_4)).

librium. These are collected in Table S6 and were used, based on the equilibria, to calculate the species present and their concentrations. To analyze the results of the spectrophotometric titrations, the extinction coefficients of the colored species $[\text{Cu}(\text{Me}_6\text{tren})(\text{H}_2\text{O})]^{2+}$ and $[\text{Cu}(\text{py})_x(\text{aq})]^{2+}$ (with $x = 1-4$) had to be established at the given conditions. Since the stability constants for $[\text{Cu}(\text{py})_x(\text{aq})]^{2+}$ had already been determined potentiometrically,¹³ the spectra of the four $[\text{Cu}(\text{py})_x(\text{aq})]^{2+}$ species could be obtained by titrating $[\text{Cu}(\text{aq})]^{2+}$ and pyridine. What emerges from these calculations is that the ternary complex ion $[\text{Cu}(\text{Me}_6\text{tren})(\text{py})]^{2+}$ possesses a spectrum that does not differ from that for the initial aqua complex, since only with this conclusion are all the data and calculations consistent and meaningful. This conclusion also provides a rational explanation of the kinetics results for addition of pyridine to $[\text{Cu}(\text{Me}_6\text{tren})(\text{H}_2\text{O})]^{2+}$, described later. Figure 4 is a speciation diagram illustrating, for a given initial aqua complex ion concentration, the formation and concentrations of other species as a function of added pyridine concentration. Figure 4 shows that, at a pH of 6.00, $I = 1.0$ M (NaClO_4), and 25.0 °C, there is a finite concentration of the ternary complex ion produced, reaching a maximum when the total pyridine concentration is 0.10 M and the complex concentration is 2.0×10^{-3} M. Simultaneously, small but not negligible quantities of $[\text{Cu}(\text{py})(\text{aq})]^{2+}$ and $[\text{Cu}(\text{py})_2(\text{aq})]^{2+}$ are being formed, and the profiles indicate the incipient presence of $[\text{Cu}(\text{py})_3(\text{aq})]^{2+}$ and $[\text{Cu}(\text{py})_4(\text{aq})]^{2+}$, which, when the total pyridine concentration is increased to 1.0 M, are practically the only species present besides the now free ligand.

Addition of pyridine to a solution of $[\text{Cu}(\text{Me}_3\text{tren})(\text{H}_2\text{O})]^{2+}$ produces similar changes in the spectrum as were noted for the tren complex. The speciation calculations were carried out using an equivalent array of parameters. One significant difference is that unlike the Me_6tren ternary complex, the complex ion $[\text{Cu}(\text{Me}_3\text{tren})(\text{py})]^{2+}$ has a different absorption spectrum from its corresponding aqua complex.

(c) Kinetic Properties. (i) Reaction of Pyridine with $[\text{Cu}(\text{Me}_6\text{tren})(\text{H}_2\text{O})]^{2+}$. The reaction of pyridine with $[\text{Cu}(\text{Me}_6\text{tren})(\text{H}_2\text{O})]^{2+}$ can be monitored kinetically in the ranges of ca. 300–350 and ca. 640–860 nm. To exploit the optimal absorbance changes, wavelengths of 330, 340, 780, 840, and 860 nm were invariably used. The rate constants obtained using an excess of pyridine did not differ when different wavelengths were employed. Rates of the reaction using total pyridine concentrations in the range of 0.020–1.0 M at a pH of 6.00 and ionic strength of 1.0 M (NaClO_4), and thus always at least in 10-fold excess over the $[\text{Cu}(\text{Me}_6\text{tren})(\text{H}_2\text{O})]^{2+}$ concentration,

Scheme 1

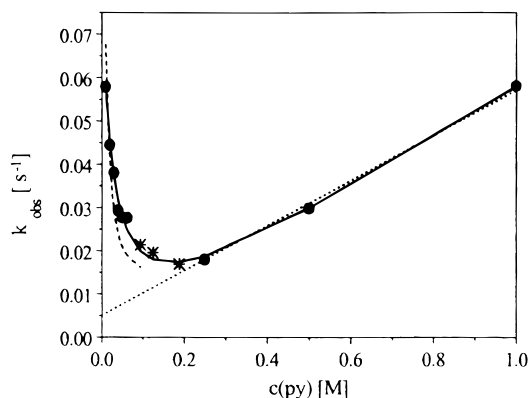
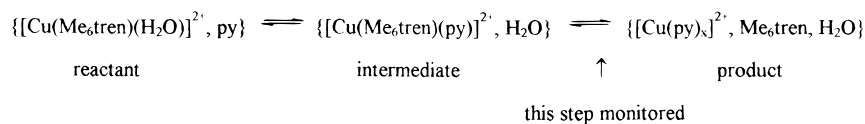


Figure 5. Kinetic data for $[\text{Cu}(\text{Me}_6\text{tren})(\text{H}_2\text{O})]^{2+} + \text{py}$ at 25.0 °C.

were such that either a conventional or a stopped-flow spectrophotometer could be used. Omission of buffer had no effect on the kinetic parameters.

Since the $[\text{Cu}(\text{Me}_6\text{tren})(\text{H}_2\text{O})]^{2+}$ and the $[\text{Cu}(\text{Me}_6\text{tren})(\text{py})]^{2+}$ complexes cannot be distinguished spectrophotometrically, the spectral changes arise due to the formation of the $[\text{Cu}(\text{py})_x]^{2+}$ species and the dissociation of $[\text{Cu}(\text{Me}_6\text{tren})]^{2+}$. The reaction itself is an equilibrium reaction, so the kinetic findings are based on that shown in Scheme 1. At low and at high pyridine concentrations we were able to fit the absorbance/time traces to one exponential function, but in the intermediate region (around 0.1 M total pyridine concentration) slight deviations from a single-exponential fit were observed. These findings may be explained in the following manner:

(1) At high pyridine concentrations, the equilibrium is driven toward products and the back-reaction is then negligible.

(2) At low pyridine concentrations, the equilibrium position is only slightly shifted; this observation can be described as a relaxation process, and it is first-order.

(3) The deviations from a single-exponential function in the intermediate concentration region arise from a contribution from second-order terms of the reverse reaction.

When k_{obs} versus pyridine concentration is plotted, k_{obs} decreases with increasing pyridine concentration in the lower concentration range, but when the pyridine concentration is increased further, k_{obs} passes through a minimum at a total pyridine concentration of about 0.1 M and then becomes linearly dependent on the pyridine concentration, as shown in Figure 5. The linear concentration dependence at higher pyridine concentrations is consistent with a simple substitution mechanism. The high pyridine concentration is driving the equilibrium position to the product side, and the contribution of the reverse reaction to the observed kinetics is negligible compared to the forward reaction. The initial decrease in k_{obs} with increasing pyridine concentration indicates a complex mechanism with more than one rate-determining step. The starred points around the minimum in Figure 5 indicate that there are small deviations from a single-exponential fit of the kinetic trace.

The following reaction paths may be considered: first, direct substitution, and second, dissociation of one chelate arm and subsequent coordination of the entering ligand. Neither of these pathways alone can explain the observed concentration depend-

ence. However, a model that includes partial dechelation as one of the rate-determining steps and direct nucleophilic attack as the other may give a satisfactory description of the kinetic results.

Studies of the kinetics of acid dissociation of $[\text{Cu}(\text{Me}_6\text{tren})(\text{H}_2\text{O})]^{2+}$ ⁸ and of substitution by anions of the coordinated water on $[\text{Cu}(\text{Me}_6\text{tren})(\text{H}_2\text{O})]^{2+}$ ^{6,25} provide additional background for understanding the pyridine substitution kinetics. The $[\text{Cu}(\text{Me}_6\text{tren})(\text{H}_2\text{O})]^{2+}$ complex ion has a trigonal bipyramidal structure and can undergo substitution either via displacement of the coordinated water molecule, or via processes after dechelation of one amine "arm" of the Me_6tren ligand. Substitution of the coordinated solvent molecule will lead to the formation of $[\text{Cu}(\text{Me}_6\text{tren})(\text{py})]^{2+}$, whereas ring opening will lead to $[\text{Cu}(\text{Me}_6\text{tren}')(\text{H}_2\text{O})]^{2+}$ in which $\text{Me}_6\text{tren}'$ denotes a tricoordinated Me_6tren . Most likely the latter dechelated species is converted rapidly to the octahedral complex ion $[\text{Cu}(\text{Me}_6\text{tren}')(\text{H}_2\text{O})_3]^{2+}$ which then undergoes rapid substitution to form $[\text{Cu}(\text{py})_x]^{2+}$ and free Me_6tren . The transition from trigonal bipyramidal to octahedral geometry is most likely to be fast because it requires only electronic rearrangements, i.e., some changes in bond lengths, but no bond breaking or bond making. We are convinced that after one arm opens the trigonal bipyramidal geometry is not retained because in this case we have in effect a parallel to a substituted diethylenetriamine (dien) which coordinates to the central atom. With such ligands typically (distorted) octahedral geometry is stabilized.¹⁹ A recent quantitative thermodynamic study of the Cu^{II} -dien system has shown that the 1:1 complex has an absorption maximum in the visible spectrum at around 600 nm, while the maximum for the 1:2 complex is shifted to lower frequencies (≈ 630 nm).²⁶ These spectral features are typical of octahedral geometry. Additionally, in a previous paper¹ we have shown that, in a given pH range, the copper complexes of 322, 332, and trpn form distorted octahedral complexes where one arm of the four-dentate ligand is not coordinated to the central atom.

In the subsequent analysis and discussion it will be shown that this is consistent with the assumption that the $[\text{Cu}(\text{Me}_6\text{tren})(\text{py})]^{2+}$ species must be in a rapidly equilibrating state with $[\text{Cu}(\text{Me}_6\text{tren}')(\text{H}_2\text{O})]^{2+}$ and with species produced in further reactions as cited above. This interpretation is compatible with the observed spectral changes which arise due to the formation of the various $[\text{Cu}(\text{py})_x]^{2+}$ species, and with the fact that the ternary complex cannot be distinguished spectrophotometrically from the aqua complex. Substitution of the axial coordinated water molecule by pyridine will probably accelerate the dechelation of the Me_6tren ligand from the copper complex ion. Two distinct paths were not observed in the substitution reaction by pyridine of $[\text{Cu}(\text{tren})(\text{H}_2\text{O})]^{2+}$, studied previously.¹⁷ In that case, the data were consistent with the formation of the ternary complex ion $[\text{Cu}(\text{tren})(\text{py})]^{2+}$ only. The difference is probably a consequence of the different metal complex stabilities.

Two mechanistic models are now proposed.

In the first model, an initial version, it is assumed that the second-order reverse reaction can be neglected under all applied

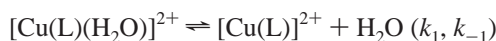
(25) Coates, J. H.; Collins, P. R.; Lincoln, S. F. *J. Chem. Soc., Faraday Trans.* **1979**, *75*, 1236.

(26) Farkas, E.; Enyadi, E'. A. Personal communications.

conditions, since the only deviations from strict first-order kinetics (in the intermediate pyridine concentration region) are small. The substitution mechanism of $[\text{Cu}(\text{Me}_6\text{tren})(\text{H}_2\text{O})]^{2+}$ consists of two parallel competing reaction paths, as indicated above. These reaction paths account for the observed kinetic data in a qualitative manner. The displacement of the coordinated solvent molecule proceeds according to a dissociative mechanism resulting in a rate law that can account for the decrease in k_{obs} with increasing $[\text{py}]$. The parallel dechelation reaction path can exhibit a linear dependence on $[\text{py}]$ with an intercept for the reverse reaction under conditions where dechelation is a preequilibrium step. The combination of these concentration dependencies will result in the curved dependence observed in Figure 5. At low $[\text{py}]$ the reaction will proceed mainly via the displacement of coordinated water, whereas at higher $[\text{py}]$ the parallel dechelation path will become more important since a linear concentration dependence is exhibited.

The reactions can be summarized as described below.

Displacement of coordinated water

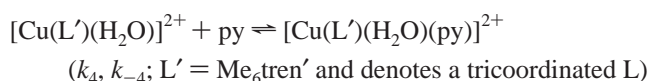
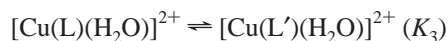


This leads to the rate law

$$k_{\text{obs}} = \frac{k_1 k_2 [\text{py}] + k_{-1} k_{-2}}{k_{-1} + k_2 [\text{py}]} \quad (1)$$

Similar nucleophile concentration dependencies have been reported for typical dissociative reactions in the literature.²⁷ Equation 1 can account for the decrease in k_{obs} on increasing $[\text{py}]$ in the lower pyridine concentration range.

Dechelation of Me_6tren

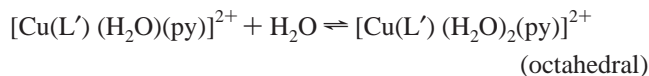
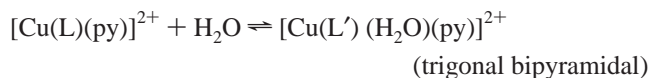


This leads to the rate law

$$k_{\text{obs}} = k_4 K_3 [\text{py}] + k_{-4} \quad (2)$$

which can in principle account for the linear increase in k_{obs} with increasing $[\text{py}]$ in the higher concentration range (Figure 5). The slope of this component of the plot is ca. $6 \times 10^{-2} \text{ M}^{-1} \text{ s}^{-1}$ and indicates that K_3 must be very small since k_4 is expected to be of the order of $10^8 \text{ M}^{-1} \text{ s}^{-1}$ if the dechelated complex is considered to be an octahedral species, i.e., $[\text{Cu}(\text{L}')(\text{H}_2\text{O})_3]^{2+}$.⁸

The following rapid equilibria combine the reaction products of the two parallel reaction paths:

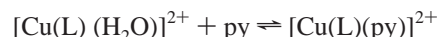
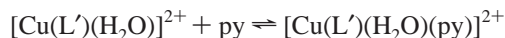
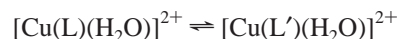


followed by the rapid displacement of L' by water and displacement of water by pyridine to produce the series of $[\text{Cu}(\text{py})_x]^{2+}$ complexes. A combination of eqs 1 and 2, as expressed in eq 3, represents a rate law with which all the data in Figure 5 can be fitted simultaneously ($k_{-4} \approx 0$).

$$k_{\text{obs}} = \frac{k_1 k_2 [\text{py}] + k_{-1} k_{-2}}{k_{-1} + k_2 [\text{py}]} + k_4 K_3 [\text{py}] \quad (3)$$

A nonlinear least-squares fit of the data according to eq 3 (see solid line in Figure 5) revealed that $k_1 \approx 0$, $k_2/k_{-1} \approx 41 \text{ M}^{-1}$, $k_{-2} \approx 0.080 \text{ s}^{-1}$, and $k_4 K_3 = 0.055 \text{ M}^{-1} \text{ s}^{-1}$. These results indicate that coordination of pyridine by $[\text{Cu}(\text{Me}_6\text{tren})(\text{H}_2\text{O})]^{2+}$ causes a significant labilization that induces the reverse (k_{-2}) aquation reaction. The competition ratio k_2/k_{-1} is quite realistic especially when k_{-1} is also converted to a second-order rate constant (k_{-1}^*), since $k_2/k_{-1}^* = 2.3 \times 10^3$.

The kinetic features discussed above can therefore be described by the following scheme in which the first two equilibria explain the decrease in k_{obs} with increase in pyridine concentration, whereas the third equilibrium relates to the increase in k_{obs} with increase in pyridine concentration:



The second model requires a more elaborate approach in which the reverse reactions (see Appendix and Supporting Information) are included. At low pyridine concentrations only a fraction of the $[\text{CuL}]^{2+}$ complex is converted into other complexes. Under such condition k_{obs} values can be treated by a chemical relaxation approach. The rate constants can be expressed as follows:

$$k_{\text{obs}} = k_1 \left(1 + \frac{\alpha}{K[\text{py}]} \right) + k_2 \left([\text{py}] + \frac{\alpha}{K} \right) \quad (4)$$

In this expression α is an equilibrium term which can be calculated point-by-point by using the method proposed by Geier *et al.*²⁸ The derivation of eq 4 is given in the Supporting Information.

At higher pyridine concentrations the conditions for the chemical relaxation approach do not prevail. Because of the coupled fast preequilibrium reactions there is a significant change in the concentrations of $[\text{CuL}]^{2+}$, $[\text{Cu}(\text{L})(\text{py})]^{2+}$, and H_xL species during the kinetic run. As a consequence some deviation is expected from the first-order kinetic behavior. The fact that at high pyridine concentrations first-order traces were observed confirms that the second-order term in eq 4, which corresponds to the reverse reaction in the rate-determining steps, is negligible. Thus the expression for k_{obs} reduces to

(27) (a) Toma, H. E.; Malin, J. M.; Giesbrecht, E. *Inorg. Chem.* **1973**, *12*, 2084. (b) Malin, J. M.; Toma, H. E.; Griesbecht, E. *J. Chem. Educ.* **1977**, *54*, 385. (c) Byers, W.; Cossham, J. A.; Edwards, J. O.; Gordon, A. T.; Jones, J. G.; Kenny, E. T. P.; Mahmood, A.; McKnight, J.; Sweigart, D. A.; Tondreau, G. A.; Wright, T. *Inorg. Chem.* **1986**, *25*, 4767. (d) Schneider, K. J.; van Eldik, R. *Organometallics* **1990**, *9*, 92. (e) Henderson, R. A.; Oglieve, K. E. *J. Chem. Soc., Chem. Commun.* **1994**, 1961.

(28) Gross, H.; Geier, G. *Inorg. Chem.* **1987**, *26*, 3044.

$$k_{\text{obs}} = k_1' = k_2'[\text{py}] \quad (5)$$

From the slope and intercept of the straight line (dotted line in Figure 5) at high pyridine concentrations: $k_1' = 6.6 \times 10^{-3} \text{ s}^{-1}$ and $k_2' = 7.0 \times 10^{-2} \text{ M}^{-1} \text{ s}^{-1}$. The substitution of these values back into eq 4 gives reasonable agreement between experimental and calculated rate constants at low pyridine concentrations (see dashed line in Figure 5).

The second model very satisfactorily accounts for the kinetic observations in the high and low pyridine concentration regions but is somewhat less successful in characterizing the intermediate concentration region, where deviations from first-order kinetics were observed, as indicated earlier.

(ii) Reaction of Pyridine with $[\text{Cu}(\text{Me}_3\text{tren})(\text{H}_2\text{O})]^{2+}$. The kinetics of the substitution of $[\text{Cu}(\text{Me}_3\text{tren})(\text{H}_2\text{O})]^{2+}$ by pyridine were studied at ambient pressure by the stopped-flow method over the pyridine concentration range from 0.02 to 0.10 M, at a pH of 7.10 ± 0.02 , and over a temperature range from 5 to 25 °C. The free pyridine concentration was calculated by using the $\text{p}K_{\text{a}}$ values of pyridine and MOPS at the given temperature. The $\text{p}K_{\text{a}}$ values of pyridine and MOPS at 25.0 °C and ambient pressure are 5.64²⁹ and 7.18,³⁰ respectively, and for pyridine they were calculated at different temperatures according to the van't Hoff equation

$$\text{p}K_{\text{a}}(T_2) - \text{p}K_{\text{a}}(T_1) = +\Delta H^{\circ} \left(\frac{1}{T_2} - \frac{1}{T_1} \right)$$

with $\Delta H^{\circ} = -5.41 \text{ kJ mol}^{-1}$,³¹ and according to Sankar and Bates for MOPS:³⁰

$$\text{p}K_{\text{a}}(T) = \frac{749.430}{T} + 5.8233 - 0.0039661T$$

with T in K.

Under all conditions the reaction was clearly first-order and, since the pyridine concentration was in large excess, the reaction is first-order in copper(II) complex ion concentration. Upon plotting k_{obs} versus pyridine concentrations a linear dependence was found, signifying a second-order rate law (see Figure S2). Derived rate constants together with kinetically determined equilibrium constants are summarized in Table S6. At 25.0 °C the second-order rate constant, k_{on} , is in the range of $4 \times 10^2 \text{ M}^{-1} \text{ s}^{-1}$; the lack of precision is a consequence of the small dependence of the observed rate constant on the pyridine concentration resulting in difficulty in obtaining the slope with precision. However, there is no doubt that the three methyl groups cause a pronounced reduction in the lability of the system, since pyridine substitutes for water on $[\text{Cu}(\text{tren})(\text{H}_2\text{O})]^{2+}$ over 2 orders of magnitude faster ($k_{\text{on}} = (1.3 \pm 0.1) \times 10^5 \text{ M}^{-1} \text{ s}^{-1}$).¹⁷ Reintroduction of water, displacing pyridine, is also retarded, but only by a factor of 4. This trend is understandable since water is a significantly more compact nucleophile than pyridine. The lack of precision of the k_{on} value precludes a definitive comparison of the kinetically and spectrophotometrically determined equilibrium constants. The agreement is within a factor of about 4, which in the absence of any evidence for intermediate formation or reason that the two measurement methods are determining a different property, reflects on the

Table 3. Kinetic Parameters for the reaction of $[\text{Cu}(\text{Me}_3\text{tren})(\text{H}_2\text{O})]^{2+}$ with Pyridine (pH = 7.10 ± 0.02 , $c(\text{MOPS}) = 0.05 \text{ M}$; $I = 1.0 \text{ M}$ (NaClO₄))

parameter	magnitude
$K_{\text{therm}} (\text{M}^{-1})$	6.6 ± 0.3
$K_{\text{kin}} (\text{M}^{-1})$	1.5 ± 0.3
$k_{\text{on}} (\text{M}^{-1} \text{ s}^{-1})$, 25.0 °C and 1.0 bar	$(4.4 \pm 0.8) \times 10^2$
$k_{\text{off}} (\text{s}^{-1})$, 25.0 °C and 1.0 bar	296 ± 5
$\Delta H_{\text{on}}^{\ddagger} (\text{kJ mol}^{-1})$	60 ± 8
$\Delta H_{\text{off}}^{\ddagger} (\text{kJ mol}^{-1})$	51.9 ± 0.9
$\Delta S_{\text{on}}^{\ddagger} (\text{J mol}^{-1} \text{ K}^{-1})$	5 ± 28
$\Delta S_{\text{off}}^{\ddagger} (\text{J mol}^{-1} \text{ K}^{-1})$	-24 ± 3
$\Delta V_{\text{on}}^{\ddagger} (\text{cm}^3 \text{ mol}^{-1})$, 25 °C	-8.7 ± 4.7
$\Delta V_{\text{off}}^{\ddagger} (\text{cm}^3 \text{ mol}^{-1})$, 25 °C	-6.2 ± 1.1

uncertainty in obtaining with high precision, parameters that are derived from the kinetic measurements.

The rapidity of the forward reaction at higher temperatures and higher concentrations of pyridine (Figure S2) adds to the problem with respect to the uncertainty in the thermal activation parameters, for the forward reaction. Nevertheless, the value of ΔH^{\ddagger} (Table 3) is much higher for the ligand exchange process (pyridine for water) system²⁹ on the $[\text{Cu}(\text{Me}_3\text{tren})(\text{H}_2\text{O})]^{2+}$ ion than in $[\text{Cu}(\text{tren})(\text{H}_2\text{O})]^{2+}$. For the reverse reaction, the thermal activation parameters are very similar to those for the comparable reaction of $[\text{Cu}(\text{tren})(\text{py})]^{2+}$, indicating a more common bonding and solvation character in the labilities of the two systems, than for the forward reactions.

At elevated pressures the temperature-jump method was used. Exhaustive examination of reference solutions allowed the conclusion that the relaxation observed must be due to a chemical process relating to pyridine/water substitution on $[\text{Cu}(\text{Me}_3\text{tren})(\text{H}_2\text{O})]^{2+}$. The reciprocal relaxation time, τ^{-1} , showed only moderate increase with increasing pyridine concentration at each applied pressure (Figure S3). Primary data were treated in the same way as was reported earlier,¹⁷

$$\tau^{-1} = k_{\text{on}}[\text{py}] + k_{\text{off}}$$

leading readily to the forward and reverse rate constants, at each pressure. For the calculation of the free pyridine concentration the protonation constants for pyridine and MOPS were corrected on the basis of the relationship

$$K^p = K \exp((-\Delta V/RT)\Delta p)$$

using previously reported reaction volumes $\Delta V = -4.4 \text{ cm}^3 \text{ mol}^{-1} (\text{py})$ ³² and $+4.7 \text{ cm}^3 \text{ mol}^{-1} (\text{MOPS})$,³³ where K , K^p , and Δp are the stability constants at 1 bar, at the actual pressure p and the difference between the two pressures, respectively.

Volumes of activation, ΔV^{\ddagger} were obtained from plots of $\ln k_{\text{on}}$ and $\ln k_{\text{off}}$ versus pressure. The plots showed no evidence of curvature, indicating that ΔV^{\ddagger} is not pressure dependent in each case, and therefore reported values refer to ambient pressure. The values are $\Delta V_{\text{on}}^{\ddagger} = -8.7 \pm 4.6 \text{ cm}^3 \text{ mol}^{-1}$ and $\Delta V_{\text{off}}^{\ddagger} = -6.2 \pm 1.1 \text{ cm}^3 \text{ mol}^{-1}$. The signal-to-noise ratio prevalent during acquisition of data used in deriving these parameters, is such that the ΔV^{\ddagger} values could not be obtained with ideal precision, especially in the case of $\Delta V_{\text{on}}^{\ddagger}$ due to the large error limits associated with k_{on} . However, the ΔV^{\ddagger} data for both reactions of the Me_3tren Cu(II) complex clearly demonstrate that the ligand exchange process follows an associative interchange (I_{a}) mechanism. Within the given error limits the ΔV^{\ddagger} data are indeed very close to those reported for

(29) Cayley, G. R.; Kelly, I. D.; Knowles, P. F.; Yadav, K. D. *J. Chem. Soc., Dalton Trans.* **1981**, 2370.

(30) Sankar, M.; Bates, R. G. *Anal. Chem.* **1978**, *50*, 1922.

(31) Martell, A. E.; Smith, R. M. *Critical Stability Constants*; Plenum Press: New York, 1989; Vol. 6, Second Supplement, p 258.

(32) Mollica, V. Z. *Phys. Chem. (Munich)* **1983**, *135*, 11.

(33) Kitamura, Y.; Itoh, T. *J. Solution Chem.* **1987**, *16*, 715.

the $[\text{Cu}(\text{tren})]^{2+}$ system, for which an I_a ligand substitution mechanism was suggested.¹⁷ It is also relevant for an explanation of our findings that Bailar³⁴ reported that the zinc complexes of the tripodal ligands 1,1,1-tris(monomethylaminomethyl)ethane and 1,1,1-tris(dimethylaminomethyl)ethane exhibited significantly different structural features. In the case of the former ligand all three amino groups coordinate to the central atom, yet in the complex of the latter ligand, due to steric influence, the ligand functions only as a bidentate chelate with one amino group not coordinated to the central zinc.

Concluding Remarks

It has been reported^{17,29,35} that substitution reactions on the trigonal bipyramidal $[\text{Cu}(\text{tren})(\text{H}_2\text{O})]^{2+}$ complex follow an associative interchange (I_a) mechanism. Upon complete methylation of the terminal amino groups, an associative substitution process on the $[\text{Cu}(\text{Me}_6\text{tren})(\text{H}_2\text{O})]^{2+}$ complex ion simple substitution does not occur due in part to steric hindrance.^{25,36} Under the experimental conditions, pyridine is able to substitute, at least partially, the tetradentate ligand.

Upon monomethylation of the terminal amino groups steric hindrance is reduced. The kinetic results and, especially the activation parameters (ΔS^\ddagger and ΔV^\ddagger) for the substitution of water in $[\text{Cu}(\text{Me}_3\text{tren})(\text{H}_2\text{O})]^{2+}$ by pyridine, indicate that the substitution process is an associative interchange (I_a) mechanism. The activation volume for the dissociation of $[\text{Cu}(\text{Me}_3\text{tren})(\text{py})]^{2+}$ is only slightly smaller than found for $[\text{Cu}(\text{tren})(\text{py})]^{2+}$.¹⁷

In fact, it is surprising that the substitution reactions of $[\text{Cu}(\text{tren})]^{2+}$ and $[\text{Cu}(\text{Me}_3\text{tren})]^{2+}$ do not differ that much

mechanistically; the monomethylation still allows an associative substitution process and the k_{on} value for the pyridine substitution process on $[\text{Cu}(\text{Me}_3\text{tren})(\text{H}_2\text{O})]^{2+}$ is ca. 10^2 times smaller than for $[\text{Cu}(\text{tren})(\text{H}_2\text{O})]^{2+}$, which in turn is far less labile than hexacoordinate aqua copper(II) ions. Upon introducing six methyl groups, the ligand substitution reaction rate is reduced by a factor of 10^5 . This may be related to a very large crystal activation energy for an I_d mechanism on trigonal bipyramidal Cu(II) complexes.³⁷

Acknowledgment. The authors gratefully acknowledge financial support from the Deutsche Forschungsgemeinschaft and the Fonds der Chemischen Industrie. They thank Dr. K. J. Wannowius (TU Darmstadt) and Dr. Z.-W. Mao (University of Erlangen—Nürnberg) for helpful discussions. F.T. acknowledges the Fonds der Chemischen Industrie for providing a research scholarship leading to a Ph.D. degree, and F.E.H. and C.O. acknowledge NATO for a Collaborative Research Grant (CRG 930121).

Supporting Information Available: Crystallographic studies and discussion of the binuclear $[\text{Cu}_2(\text{Me}_3\text{tren})_2(\text{CN})](\text{ClO}_4)_3 \cdot 2\text{CH}_3\text{CN}$ complex, tables of atomic coordinates, complete bond distances and angles, thermal parameters and derivation of the quantitative model, and three figures (an ORTEP diagram and two kinetic plots) are available (19 pages). Ordering information is given on any current masthead page. Crystallographic data (excluding structure factors) for the structure reported in the paper have been deposited with the Cambridge Crystallographic Data Centre as supplementary publication no. CCDC 102108. Copies of the data can be obtained free of charge on application to the Director, CCDC, 12 Union Road, Cambridge CB2 1EZ, UK (fax, +44 (1223) 336-033; e-mail, deposit@chemcrs.cam.ac.uk).

IC971295T

(34) Kasowski, W. J.; Bailar, J. C., Jr. *J. Am. Chem. Soc.* **1969**, *91*, 3212.

(35) Cayley, G.; Cross, D.; Knowles, P. *J. Chem. Soc., Chem. Commun.* **1976**, 837.

(36) Lincoln, S. F.; Coates, J. H.; Doddrige, B. G.; Hounslow, A. M.; Pisaniello, D. L. *Inorg. Chem.* **1983**, *22*, 2869.

(37) Lincoln, S. F.; Hounslow, A. M.; Pisaniello, D. L.; Doddrige, B. G.; Coates, J. H.; Merbach, A. E.; Zbinden, D. *Inorg. Chem.* **1984**, *23*, 1090.